



---

## A Simple Electrostatics Model for Nanotube/Metal Junction

---

**Z. Chen<sup>a</sup>**

<sup>a</sup> *Lava Education  
930 Roosevelt, Suite 232, Irvine, CA, United States 92620  
E-mail: [zzchen@lava-edu.com](mailto:zzchen@lava-edu.com)*

**ABSTRACT:** Making good Nanotube/Metal contact is one of the key requirements in making better performance nanotube electronics. We propose a simple electrostatic model, whose parameters are benchmarked against more sophisticated ab initio simulations, and studied the effects of the nanotube diameter on the quality of the contact. We found that the small effective contact area associated with small diameter tubes limits the injection of holes into the nanotube and deteriorates contact quality. The critical diameter for barrier free injection is  $\sim 1.6$  nm, which agrees well with experiments. An experimental approach is proposed to verify the correctness of the model and determine the nature of the Nanotube/Metal heterojunction.

**KEYWORDS:** NANOTUBE; INJECTION; SCHOTTKY BARRIER.

### 1. Introduction

Carbon Nanotube field-effect transistors (CNTFETs) have many attractive features for future nanoelectronics, like its small size, structural stability, higher mobility and mature synthesis methods. Its capabilities and performance have already been demonstrated.<sup>1,2</sup> Wind et al<sup>3</sup> showed that electrical characteristics of CNTFET are comparable or exceeds the performance of conventional MOSFET. Many progresses are being made in understanding the working mechanism of CNTFETs<sup>2,4</sup> and optimizing the relevant device structure<sup>5</sup>.

The working mechanism of the CNTFET is still under heated debate, which boils down to the understanding of the Nanotube/Metal junction. Depending on the nature of the junction, The CNTFET can operate either in a way similar to conventional MOSFETs<sup>1</sup> or as a Schottky Barrier (SB) transistor<sup>4</sup>. There have been many transport experiments trying to identify the nature of the contact. Most previous work reported Schottky type contact<sup>6</sup>. Recently, some progress has been

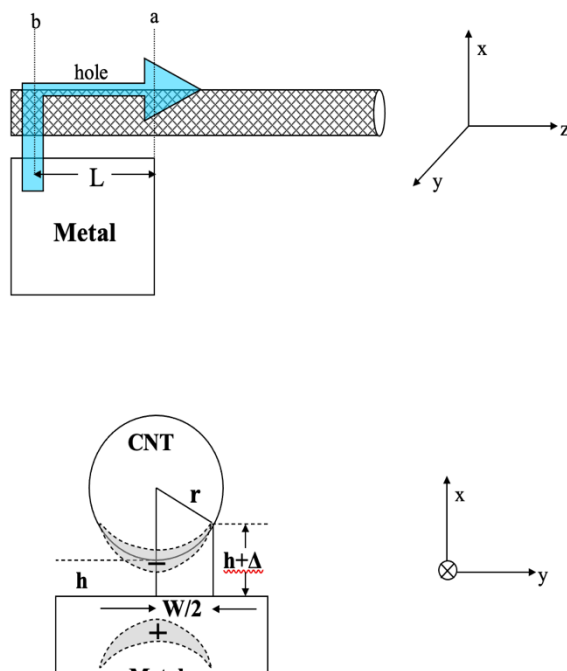


**Figure 1.** Side view and cross section view of the Nanotube/Metal junction geometry. a) Schematic picture of the path for hole injection. The hole injected at a position that is of distance  $L$  from the edge, then travels along the top surface into the channel region. b) Cross sectional view of the Nanotube/Metal junction. The dipole layer is model by a sheet of charge on the nanotube and its corresponding image charge in the metal, which is the shaded region on the graph. The shape of the shadow indicates the surface charge density.

made in achieving good ohmic contacts. Pd was found to make good ohmic contact to nanotubes<sup>1,7</sup>. Good ohmic contact was also achieved by using Au AFM tip as contact metal<sup>8</sup>. However, up to now, ohmic junction has only been achieved in relatively large CVD grown nanotubes. Smaller diameter nanotubes fabricated by laser ablation<sup>9</sup> or HiPCO<sup>10</sup> techniques (0.8~1.5 nm) are always found to exhibit Schottky behavior. This has been previously attributed to the lower effective mass associated with larger tubes and preferable band lineup<sup>11</sup>. We point out here that, besides these preferable conditions, the specific geometry related associated with side contact junction also helps to reduce the Schottky Barrier. We propose a simple electrostatic model whose parameters are benchmarked against more sophisticated *ab initio* calculations and studied the effects of nanotube diameter on the contact quality. We found the effective contact length for small diameter tubes is much smaller, usually by a factor of ten, than the actual experimental contact length. This limits the possible injection area for holes and seriously deteriorates contact quality. The critical diameter below which this happens is  $\sim 1.6$  nm.

## 2. Models and Methods

The model we propose for the Nanotube/Metal junction is sketched out in Figure 1a. The nanotube is side contacted to the metal electrode, and the arrow indicates a characteristic path for the hole injection. The potential barrier the hole sees along this path is representative of its ease of injection into the channel region. A dipole layer is formed between the nanotube and the metal surface from  $(-\infty, 0]$  in Z direction. The width of the dipole is taken to be  $\sqrt{r^2 - (r - \Delta)^2}$  in Y direction as indicated on Figure 1b. From previous ab initio simulations, the net charge is mainly localized at the interface and only spills several carbon atoms into the nanotube. Thus, we take  $\Delta = 3\text{\AA}$  to be the cut off height, above which the C atoms are charge neutral. The surface charge density within height  $[h, h + \Delta]$ , as well as its corresponding image charge in the metal, takes the exponential form  $\sigma = \sigma_0 e^{-qx}$ , which correctly captures the picture of Metal Induced Gap States (MIGS).<sup>12</sup> The final potential profile is a superposition of the bare bands lineup plus the potential due to the interfacial dipole moment. Band bending due to space charge is taken to be flat on the length scale we consider here. In Ref 8, Park et al saliently pointed out that end contact geometry is indeed possible and shows novel physical properties. However, we adopt the side contact geometry here for two reasons: 1) In some experiments, it is difficult to determine experimentally the contact geometry because of the buried interface<sup>1</sup>, in some other experiments, the nanotubes are side contacted to the metal<sup>13</sup>, the AFM tip contact case is a concrete example of side contact<sup>8</sup>. Therefore, side contact geometry is relevant and important. 2) In the end contact geometry case, the dipole decays away quickly due the reduced dimensionality and the resulting Schottky barrier is not sensitive to tube diameter. The end contact model does not account for the experimental observation that only larger diameter tubes make good ohmic contacts.<sup>14</sup>

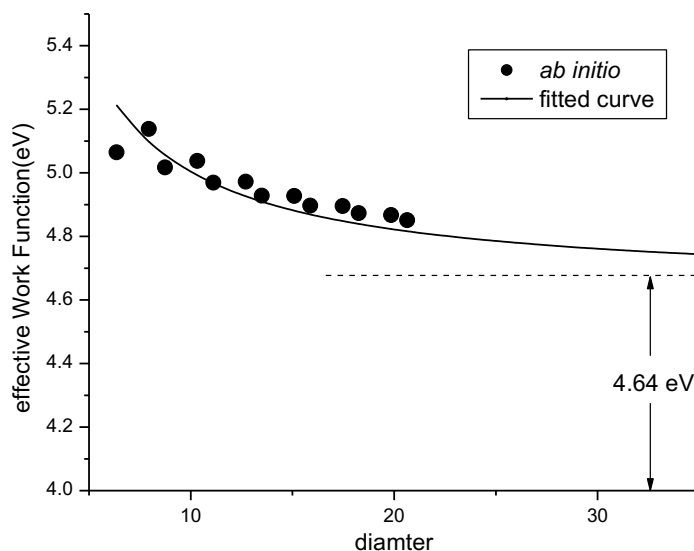


**Figure 2.** Effective work function defined as the energy difference between the vacuum level and the valence band top. The dots are from ab initio calculations, and the solid line is a curve fit of the form  $y = A/d + 4.64$  eV, with  $A = 3.6$  eV·nm.

In this simple electrostatic model, the parameters are estimated or fitted to *ab initio* calculations. The equilibrium distance is set to be 2.0 Å, where *ab initio* calculations indicate the distance between different nanotube/metal varies from 1.8 – 2.2 Å. The work function of the metal is set to 5.6eV, which is also obtained from *ab initio* calculations for a Pd (111) surface. The surface charge density at the interface  $\sigma_0$  is a fitting parameter and is determined such that it gives the correct band lineup for (8,0) CNT and Pd (111) surface. The details of the band lineup calculation can be found in Ref. This charge density is kept constant and used throughout all the calculation. Doing so, we neglected the charge density difference between different diameter nanotube metal combinations. However, we expect this fluctuation to be small and do not change our conclusion. We note that if we assume the charge density increases linearly with work function difference, the general picture still holds, while the estimated critical diameter will increase a little bit. Since we lack a benchmark calculation that takes this into account, we have fixed it as a constant throughout our study. Another important piece of information is the *unpinned* band lineup for the metal and tube. For this purpose, we have calculated the effective work function, defined as the potential difference between the valence band top and the vacuum level, of nanotubes from 8 Å to 2 nm using *ab initio* planewave pseudopotential method. Figure 2 shows the calculated work function with respect to the tube diameter for (n, 0) semiconducting nanotube. The data is fitted to a curve of the form  $y = \frac{A}{r} + B$  to get an estimate of the workfunction for tubes of various diameters. B in the above formula is the work function for infinitely large diameter tube. It should asymptotically approach the work function of a single graphene sheet, which is 4.64 eV from our *ab initio* calculation.

### 3. Results and Analysis

Figure 3 shows the potential profile along the path for a hole when it is injected from a position  $L = 4$  nm from the edge point a. The metal Fermi surface is set to zero on the graph. The curves show the potential profile for tubes of diameter 1.2 nm, 1.6 nm and 2.2 nm respectively. The barrier right next to the metal is associated with the barrier of injection from the metal into the nanotube. The barrier decays off because the hole travels along the circumference of the nanotube and gets away from the interfacial dipole. Modeling the height and shape of the barrier within this region is not quite accurate due to the possible distortion in electronics structure at the interface. But this barrier is usually thin and does not dominate the tunneling process. The following plateau after the barrier corresponds to the potential the hole sees when it travels along the top surface of the nanotube from the injection point to the channel region. It is indeed this process that dominates the probability of hole injections. As can be seen from the graph, the associated barrier is larger for a smaller diameter nanotube than a larger diameter one. As the diameter of the tube increases, the barrier gradually diminishes. This is due to the particular geometry of the side contact. After the hole is injected into the CNT, it tends to propagate to the place where the potential is lower (for the hole), which is the top surface of the CNT. However, small diameter nanotubes put geometrical constraint on how far away the holes can go on the XY plane. For small diameter tubes, this barrier exists in spite of the fact that the electron moves as far away as possible in the XY plane. In subsequent propagation into the channel region, this barrier almost remains constant and severely limits the hole injection. The diameter where this barrier effectively becomes zero happens at 1.6 nm, which is in very nice agreement with experimental observations. As the hole propagates through the edge point a, dipole moment at the surface dies out and the valence band tends to approach its unpinned position, which is just the effective work function we defined above.

From the above discussion, we see that for nanotubes with diameters less than 1.6 nm, the holes would prefer to inject from the edge point  $a$ , as this path minimizes the potential barrier to overcome. Figure 4a shows the potential profile for electrons injected from metal to (8,0) CNT with different  $L$ . The tunneling probability decreases rapidly as  $L$  increases. We define an

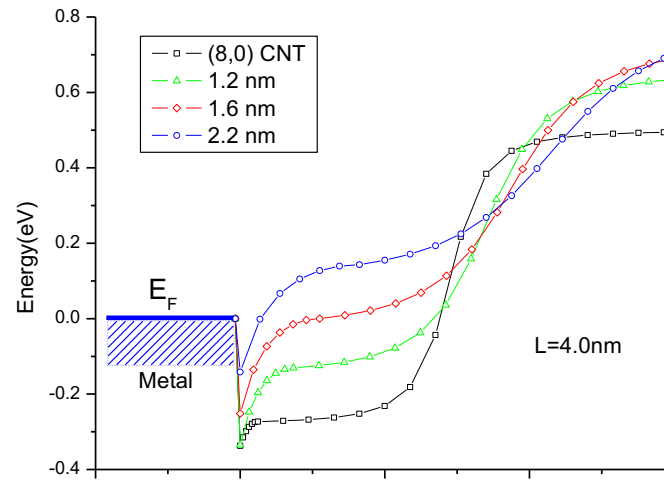


**Figure 3.** Potential profile along hole injection path for nanotube of different radius.

effective contact length, from where the hole has a tunneling probability of  $1/e$  traveling along the top surface of the nanotube into the channel region. The tunneling probability is calculated using WKB approximation. Figure 4b shows the effective contact length as a function of tube diameter. We see the effective contact length is only several nm for small diameter nanotube and increases rapidly around 1.6 nm, which means there's little difference for holes to be injected with different  $L$ . This has important implications. In the actual experiment, the metal finger contacting the tube is usually  $\sim 250$  nm in size. In AFM tip contacted devices, the contact length is also on the order of 40 nm. However, for small diameter nanotube, the actual physical contact area is irrelevant. The injection of holes is limited to only within several nm from edge. This is a huge reduction in contact area. Any defect or weak bonding at the interface may block the hole injection and deteriorate contact quality.

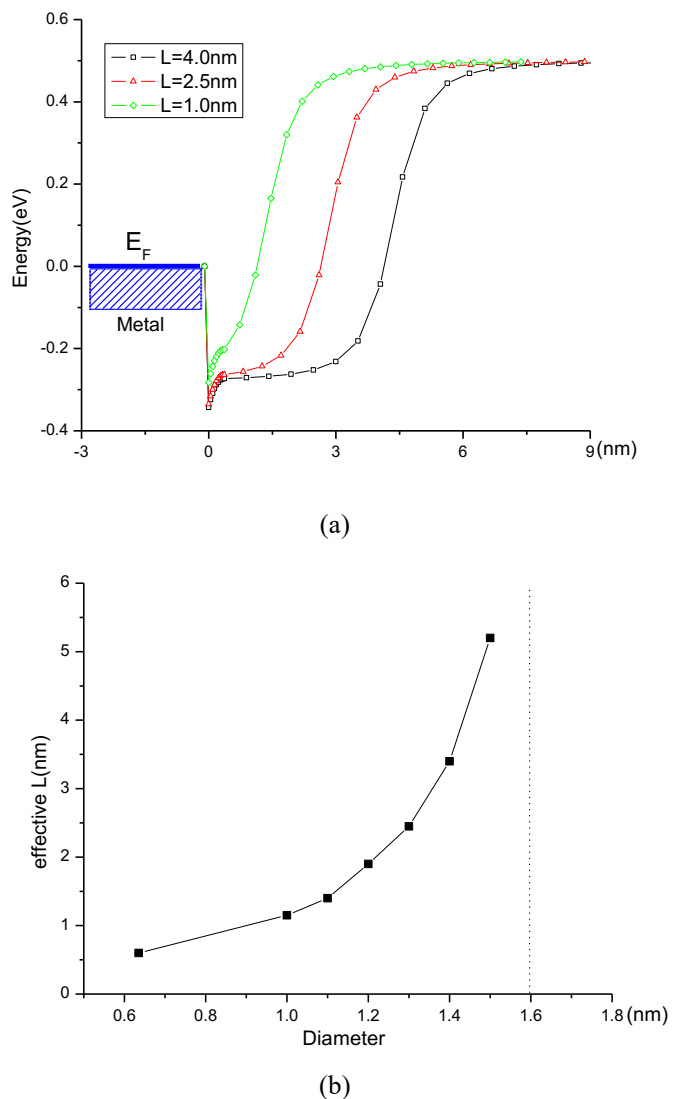


**Figure 4.** (a) Potential for holes injected at  $L=4\text{nm}$  from the edge. (b) Effective tunneling length as a function of tube diameter.

From our previous discussion, we propose a way of experimentally verifying the correctness of the model and probing the nature of the metal/nanotube junction. The idea is to determine the injection position of the electron into the nanotube. We can determine the size of the tube resonator or dot by the low  $T$  transport measurements (FP and CB oscillations). The metal gap can be measured separately from any microscopy tools like AFM or STM. For Schottky Barrier devices, these two would match since the electrons are much more likely to be injected from the edge. For true ohmic contact, it makes less difference where the electrons are injected, so the measurements from step one would be larger than step two.

#### 4. Conclusion

In conclusion, we have developed a simple electrostatic model which is benchmarked against *ab initio* calculations. This simple model gives insight into the role of tube radius on the contact quality. The scaling behavior of the Schottky barrier is found to be different from either the bulk case or the end contact case. The predicted critical diameter is in good agreement with experiments. An experimental setup is also proposed to verify the correctness of the model. An understanding of the Nanotube/Metal junction helps optimize nanotube electronics.

#### Acknowledgments

This work is supported by NSF grant on Network for Computational Nanotechnology. We thank Ali Javey and Hongjie Dai for sharing experimental details and helpful discussions.

#### References

- [1] Jing Guo Ali Javey, Qian Wang, Mark Lundstrom & Hongjie Dai, *Nature* **424**, 654 (2003).
- [2] J. Appenzeller, J. Knoch, R. Martel, V. Derycke, S. J. Wind, Ph. Avouris., *IEEE Trans. Nanotechnology* **1** (4), 184 (2002).
- [3] J. Appenzeller, S. J. Wind, R. Martel, V. Derycke, Ph. Avouris, *Appl. Phys. Lett.* **80**, 3817 (2002).
- [4] S. Heinze, J. Tersoff, R. Martel, V. Derycke, J. Appenzeller, and Ph. Avouris, *Phys. Rev. Lett.* **89**, 106801 (2002).
- [5] J. Tersoff S. Heinze, and Ph. Avouris, *Appl. Phys. Lett.* **83**, 5038 (2003).
- [6] J. Appenzeller, J. Knoch, V. Derycke, R. Martel, S. Wind, and Ph. Avouris, *Phys. Rev. Lett.* **89**, 126801 (2002)
- [7] A. Javey, D. Mann, J. Kong, Q. Wang, H. Dai, *Nano Lett.* **3**, 1542 (2003).
- [8] J.-Y. Park Y. Yaish, S. Rosenblatt, V. Sazonova, M. Brink, P. L. McEuen, *Phys. Rev. Lett.* **92**, 046401 (2004)
- [9] Y. Yaish S. Rosenblatt, J. Park, J. Gore, V. Sazonova, P. L. McEuen, *Nano Lett.* **2**, 869 (2002).
- [10] R. Lee A. Thess, P. Nikolaev. H. Dai, P. Petit, J. Robert, X. Chunhui, L. Y., Hee, K. Seong Gon, A. G. Rinzler, D. T. Colbert, *Science* **273**, 483 (1996).
- [11] Ph. Avouris, M. Radosavljević, S. J. Wind, *Carbon Nanotube Electronics and Optoelectronics*. In: S. Rotkin, S. Subramoney (eds) *Applied Physics of Carbon Nanotubes. NanoScience and Technology*. Springer, Berlin, Heidelberg. (2005).
- [12] F. Léonard, J. Tersoff, *Phys. Rev. Lett.* **84**, 4693 (2000).
- [13] M. Bockrath, D. H. Cobden, P. L. McEuen, *Phys. Rev. Lett.* **81**, 681 (1998).
- [14] Q. Wang, A. Javey, W. Kim, H. Dai, *International Electron Devices Meeting Technical Digest*, 741 (2003).